Mathematical Modelling of Weld Phenomena 9, eds. H. Cerjak and N. Enzinger, TU-Graz, pp. 997-1010, 2010.

EXPERIMENTAL AND NUMERICAL ANALYSIS OF THE HOT TEARING SUSCEPTIBILITY OF A CuCrZr ALLOY

J.-M. DREZET*, D. AYRAULT**, J. WISNIEWSKI**,***
P. PILVIN***, D. CARRON*** and F. PRIMAUX****

**Ecole polytechnique Fédérale de Lausanne, LSMX, station 12, CH-1015 Lausanne, Switzerland*
*** Commissariat à l'Energie Atomique, CEA/DEN/DM2S/SEMT/LTA - Bt 611, GIF SUR YVETTE, F-91191, France*
**** Université de Bretagne Sud, LIMATB, Rue de St Maudé, LORIENT, 56321, France*
***** Le Bronze Industriel, Z.I. Voie de Châlons, RD 977, SUIPPES, 51600, France*

ABSTRACT

The precipitation hardened CuCrZr alloy is used in fusion machines for the heat sink of intensely cooled plasma facing components (PFC) due to its good thermal and mechanical properties. Albeit, the feedback from its application in Tore Supra (French tokamak) showed that this alloy is very sensitive to hot tearing during electron beam welding. Hot tears also known as solidification cracks occur in solidifying parts undergoing tensile stresses that are transmitted to the mushy zone by the coherent solid underneath.
In order to characterize the hot tearing susceptibility of the CuCrZr alloy, welding tests based on the investigations of the Joining and Welding Research Institute (JWRI) have been performed. Electron beam fusion lines are performed on a thin rectangular plate equipped with thermocouples and firmly clamped at its extremity in the vacuum chamber. As the width of the plate decreases, conditions leading to the formation of hot tears appear in the run-in, thus defining a critical width hot tearing wise.
The JWRI welding tests are then analysed by means of numerical modelling and available hot tearing criteria. To do so, missing thermophysical and thermomechanical properties are determined by associating laboratory tests and numerical analysis. The viscoplastic strain and viscoplastic strain rate undergone by the solidifying alloy are considered as hot tearing (HT) indicators. Critical values at the onset of hot tearing are determined for this particular alloy. In addition, HT initiation conditions are compared with propagation conditions using a simple numerical approach.

I INTRODUCTION

The precipitation hardened CuCrZr alloy is a potential candidate for use as a heat sink of the first wall components for the future thermonuclear fusion reactor ITER [1] owing to its good mechanical and thermal properties. The feedback from its use in Tore Supra [2] showed that this alloy is very sensitive to hot tearing (solidification cracking) during electron beam welding. Different cracking tests [3-7] have been developed in the past and most of them consist in performing a fusion line on a thin specimen in order to generate a hot crack. However, the specimen shape is varying according to the authors such as rectangular shape

[3-4], with a fusion straight-line in the middle of the specimen [3] or an oblique one [4], and fan shape [5-7], inspired by the Houldcroft test [5]. For the latter test [7], the fusion line is made from the smallest width of the specimen which allows the occurrence of a hot crack till the biggest one for which the initiation conditions are not encountered. In order to characterize the hot tearing susceptibility of the alloy and thus define acceptance tests for various supplies, a laboratory test, inspired by the work carried out at the Joining and Welding Research Institute (JWRI) by Shibahara et al. [3] is used in the present investigation.

From the physical point of view, hot tearing has been recently deeply studied as it remains one of the major defects that can occur during solidification of an alloy. This defect is the result of inadequate melt feeding initiating tears and severe deformation leading to the opening and propagation of the tears. This type of defect appears at the end of the solidification when the solid fraction is high [8-10]. Two main mechanisms associated with hot tearing are the solidification shrinkage leading to interdendritic melt flow and the thermally induced deformation caused by non uniform cooling contraction of the metal at the rear of the weld pool [11]. Many criteria have appeared with more or less success. A review of the literature on the subject over the last 50 years has been published by Eskin et al. [12]. Among the available criteria, the RDG (Rappaz-Drezet-Gremaud) [8,13] hot tearing criterion considers both the solidification shrinkage and the mechanical straining of the mushy zone. If the flow of interdendritic liquid cannot compensate for the local change of volume, a void may form and give rise to a crack. Performing a mass balance over the liquid and solid phases, the criterion takes into account the tensile deformation of the solid skeleton perpendicularly to the growing dendrites and the feeding by the interdendritic liquid [13]. The maximum strain rate sustainable by the mushy zone at the root of the dendrites before a hot tear forms can be derived. In other words, the larger the strain rate undergone by the mush is, the larger the risk to form a crack. This is valid when continuous liquid films are still present and grains have not yet fully coalesced, that is at solid fractions higher than approximately 95 % [10]. The interval of temperatures where continuous liquid films exist can be considered as the brittle temperature range (BTR) [14-15]. This interval goes from the zero strength temperature (ZST) below which a continuous liquid film exists around the dendrites (incoherent network) but liquid feeding is almost impossible owing to the very low permeability of the medium, and the zero ductility temperature (ZDT) at which dendritic bridging or coalescence [16] occurs and increases the macroscopic ductility of the medium that can now withstand some tensile loadings. The minimum in the U ductility curve is a crucial parameter as it limits the strain the mushy zone can sustain without creating a crack. Kerrouault [17] measured a minimum of ductility between 0.5 and 1% at 1410°C for the AISI 321 austenitic stainless steel with the help of Varestraint and JWRI tests. Similarly, Cerri [18] used a value of 1% for two different steels, 40CrMnNiMo8 and 100Cr6. No values for copper based alloys were found in the literature.

Hot tearing remains an important subject of research, notably with the computation of liquid feeding using Kirchhoff-Poiseuille models and strain localisation [19]. As the strain rate acting over the mush is of high importance hot tearing wise, the main challenge is to

establish a reliable constitutive model for the mechanical behaviour of the welded material. Although the mush should be treated as a compressible medium with the help of internal variable models [20], a simple incompressible model is adopted here for sake of simplicity. Indeed, many mechanical tests in the solidification interval are required to determine the numerous parameters describing the compressibility of the mushy alloy [21].
The purpose of the present study is to assess the mechanical loading in terms of deformation and strain rate that leads to hot tearing initiation at the rear of the weld pool. For this aim, JWRI tests are analysed together with a numerical model built in Abaqus 6.8. The initiation conditions are then compared to propagation conditions determined numerically.

II EXPERIMENTAL INVESTIGATION

JWRI tests [3] as described in the previous section are carried out with the precipitation hardened CuCrZr alloy. The alloy composition complies with the DIN 17672 standard with Cr content between 0.5 and 1.2 wt pct and Zr content between 0.03 and 0.3 wt pct. [22]. Electron beam fusion lines are performed in a vacuum chamber on thin rectangular plates 2,5 mm in thickness instrumented with thermocouples. The welding parameters are kept constant throughout all the tests: speed is 50 cm/min, tension is 50 kV, intensity is 70 mA and focal distance is 20 mm above the plate. These parameters yield a nominal heat input of 3.5 kW. Fig. 1 shows the experimental set-up used for the JWRI welding tests [22].

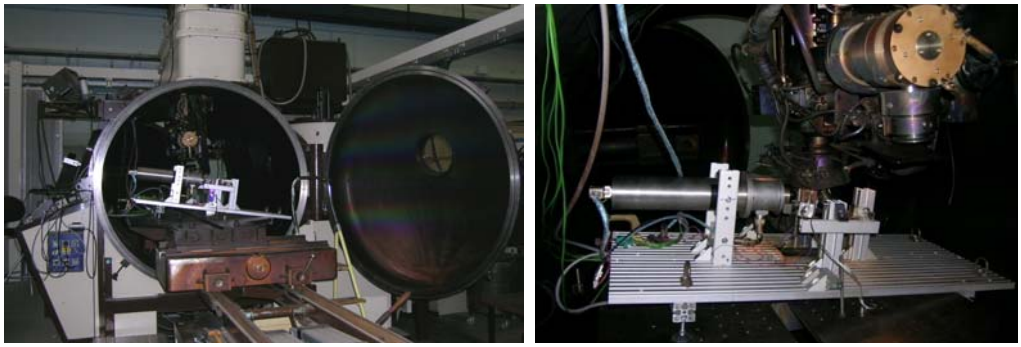

Fig. 1: experimental set up used for the JWRI tests; vacuum chamber on the left and electron canon together with welding table on the right [22].

The plates were machined out from billets 100 mm in diameter. Those billets were cast and provided by Le Bronze Industriel (LBI) after they undergo a precipitation hardening thermal treatment. Fig. 2 shows the geometry of the plates with the minimum (30 mm) and maximum (78 mm) width. Please note the presence of an appendice that is supposed to enhance the conditions for hot tearing at run-in because it falls down when passing the beam. On the left hand side, the plate is firmly fixed with the help of a clamping device. The electron beam is travelling from the right to the left at the constant speed over a distance of approximately 60 mm [22]; this takes 7.2 s.

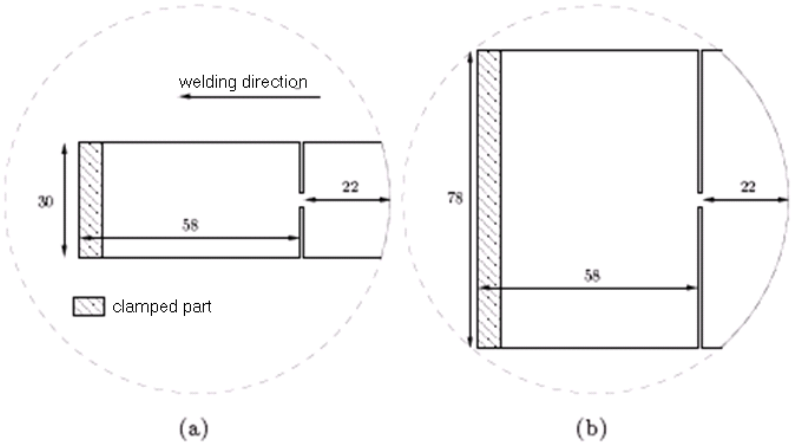

Fig. 2: geometry of the JWRI test samples machined out in billets: a) 30 mm width, b) 78 mm width [22].

Fig. 3 shows two top views filmed during the JWRI tests. A hot tear is visible in the 30 mm wide plate whereas the 78 mm wide sample is sound. Note also that the pool size decreases a little as width increases going from 4.7 x 6 mm^2 at 30 mm to 4.5 x 5.3 mm^2 at 78 mm.

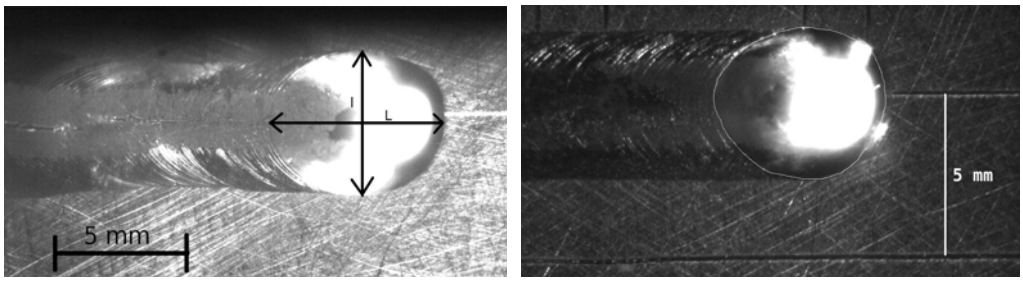

Fig. 3: top view images filmed during the JWRI tests: left) 30 mm wide plate exhibiting a hot tear along the fusion line, right) 78 mm wide plate.

Fifteen JWRI tests were carried out using exactly the same welding parameters but with different plate widths. Similar tests were repeated to check the reproducibility of the results. Table 1 gives the number of cracking occurrence as a function of the width of the plate. As width decreases from 78 mm down to 30 mm, a crack appeared. Hot tear always appeared in the run-in regime right after the appendice has fallen down. Moreover, the crack always followed the weld line, as shown in Fig. 3 (left image). The cracking at a width of 60 mm should be ignored as for that particular trial the plate thickness was lower than 2.5 mm thus altering the test conditions. The 50 mm wide plates yielded two cracked samples and two sound ones; this width is therefore considered as the critical width hot tearing wise. Fig. 4 shows the scanning electron microscopic analysis of two samples, 30 and 78 mm in width. The coarse microstructure present in the weld pool is comparable in both test samples and

the hot tear remains along the weld axis. The next section gives details on the material properties that are required for the numerical analysis of the JWRI tests.

width (mm)	Cracking	No cracking
30	3x	
40	3x	
50	2x	2x
60	1x (plate thickness 2.32 mm)	1x
78		3x

Table 1 hot tearing occurrence as a function of the plate width.

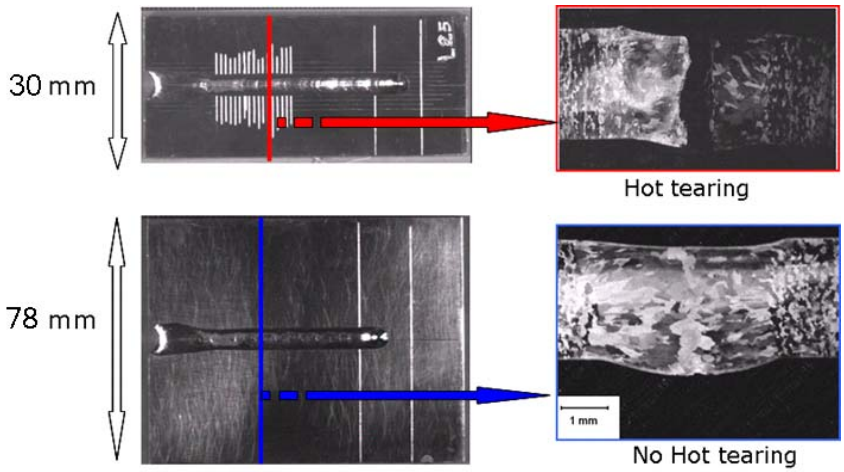

Fig. 4: 30 and 78 mm wide test samples: top) 30 mm wide plate exhibits a hot tear, bottom) 78 mm wide plate is sound.

III MATERIAL DESCRIPTION

To carry out the finite element analysis, it is necessary to know not only the mechanical behaviour from liquid state down to room temperature but also the thermophysical properties of the alloy. The missing physical properties were determined by associating laboratory tests and numerical analysis and are reported in [23]. Fig. 5 presents the thermal conductivity and the solidification path (solid fraction versus temperature) of the CuCrZr alloy under investigation. The solidification path retained for the present analysis is based on the Scheil-Gulliver model owing to the very high cooling rate present at the rear of the weld

pool. This model gives a solidus and a liquidus temperature of 1048°C and 1080°C, respectively. The solidification interval is thus only 32°C. The fusion latent heat of the CuCrZr alloy is assumed to be that of pure copper (204 kJ/kg) owing to the low content of alloying elements.

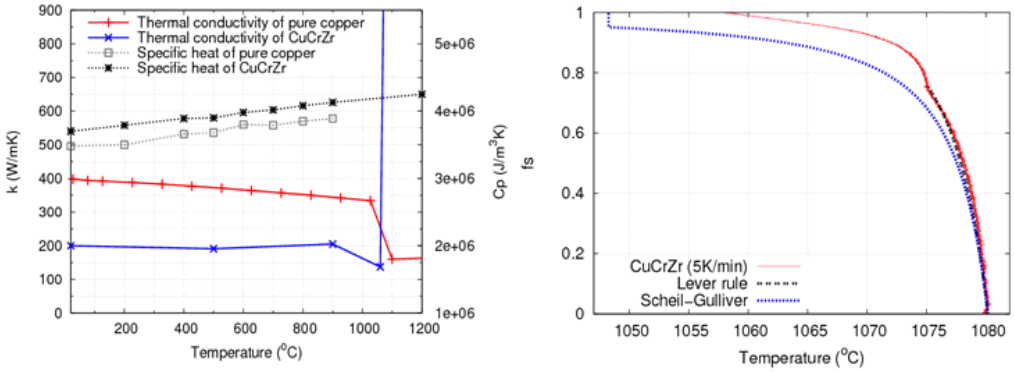

Fig. 5: thermophysical properties of the CuCrZr alloy: left) thermal conductivity and specific heat, right) solidification path [23].

The mechanical properties of the CuCrZr alloy were measured with the help of a Gleeble 3500 machine at Université de Bretagne Sud (UBS) at temperatures ranging from 250°C to 1000°C [24]. Some mechanical tests were also performed at 20°C with an Instron 30 machine. Tensile tests were carried out at different strain rates. The measured curves were then simulated with an elasto-visco-plastic (EVP) constitutive model assuming that the material behaviour was isotropic, restoration was negligible and the deformation was made out of three components, elastic, thermal and viscoplastic. By imposing temperature variations to the Gleeble specimen, the thermal linear coefficient was determined at different temperatures. In addition, the temperature dependence of the Young's modulus and the Poisson's ratio were also determined. Finally, the viscoplastic strain rate is given by the following isotropic hardening law [24]:

$$\dot{\varepsilon}_{vp} = \left(\frac{\sigma_{eq} - \sigma_y - Q(1 - e^{-b\varepsilon})}{K} \right)^n \qquad (1)$$

where K is the consistency of the alloy, ε is the accumulated viscoplastic strain, σ_{eq} is the Von Mises equivalent stress, σ_y is the yield stress, n is the stress exponent and Q and b are parameters that describe the hardening of the alloy. This law requires the knowledge of five parameters that are all temperature dependent and that were determined by inverse method with the help of the Sidolo software [25]. The comparison of the measured and modelled curves is presented in Fig. 6 for temperatures ranging from 600°C to 1000°C [22, 24]. All these parameters were used in the numerical analysis of the JWRI weld tests.

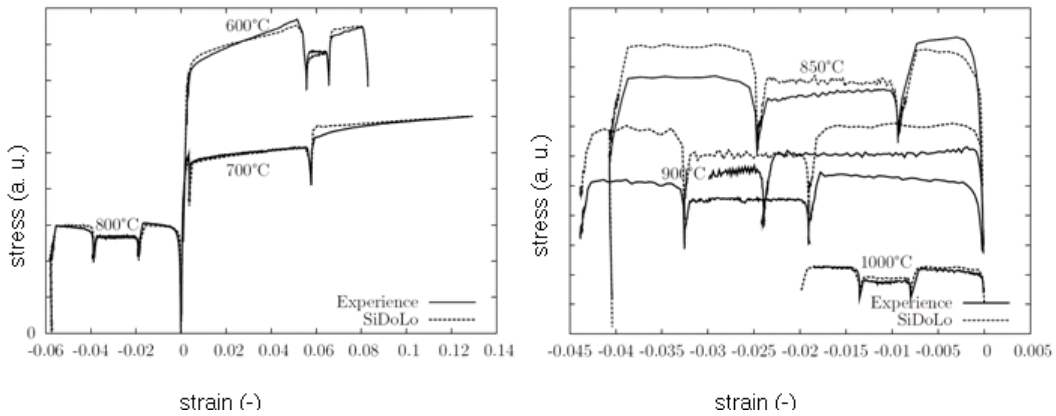

Fig. 6: comparison between the measured curves and the results obtained with the EVP model [22, 24].

IV FINITE ELEMENT NUMERICAL ANALYSIS

As stated in the introduction, the hot tearing sensitivity is linked to the mechanical loading undergone by the alloy during solidification at the rear of the liquid pool. The present section provides details on the finite element (FE) model used to assess the strain and strain rate levels at the onset of hot tearing. The model is built in Abaqus 6.8.

As thin plates were used for the welding trials and fusion was fully penetrating (cf. Fig.4), it is assumed that the temperature field does not vary much through the thickness. Therefore a 2D model is used. Only half the plate is modelled owing to the symmetry plane. The mesh for a half specimen width of 15 mm is presented in Fig. 7. In the FE analysis, only the dimension along y, i.e., the half width of the plate, is varying. The electron beam is supposed to travel along the x-axis from the left to the right and the mesh is refined (200 x 200 microns) in the regions that undergo melting and solidification. The length of the domain (60 mm, dimension in x) was used so that the transient run-in and run-out regimes are well separated by a steady state regime in the so-called on-going zone.

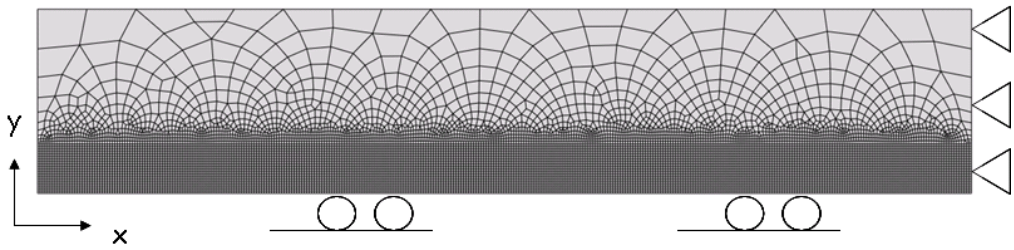

Fig. 7: FE mesh used for the present study together with the mechanical constrains.

The electron beam heat input imposes a high local heating of the sample. The temperature field is modelled by the steady state Rosenthal 2D equation valid for thin plates [26]:

$$T(x,y) = T_0 + \frac{\beta P}{2ks}\sqrt{\frac{\alpha}{\pi V r}}e^{-\frac{V}{2\alpha}(x+r)} \quad \text{with} \quad r^2 = x^2+y^2 \qquad (2)$$

where k is the thermal conductivity of the alloy, V the welding speed (50 cm/min), α the thermal diffusivity (34.75 mm^2/s), s the plate thickness (2.5 mm), P the nominal power (3.5 kW) and β the absorption coefficient. When r approaches 0, the Rosenthal function T(x,y) is set to 1100°C, 20°C above the liquidus temperature of the CuCrZr alloy. The absorption coefficient is adjusted so that the computed weld pool size matches the average measured one (4.6 mm in width and 5.65 mm in length). A value of 83 % is found which is typical of EB welding owing to the formation of plasma in the fusion pool. Along the welding axis, the thermal gradient at the solidus temperature, Gx, is of very high importance when treating the problem of hot tearing initiation [10]. This quantity is calculated analytically using Eq. 2, Gx = 124 K/mm. Similarly the cooling rate at solidus temperature given by – Gx.V equals -1033 K/s. Those two quantities are constant throughout the present study as neither the welding speed nor the beam power changes. As the mechanical field is considered to have no influence on the thermal field, at least before any crack initiates, the thermo-mechanical computation is uncoupled. Therefore, the thermal field given by Eq. 2 is calculated by moving the electron beam along the direction x by a quantity Vdt for a given time step dt. This thermal field is then used as a loading for the mechanical calculation.

As shown in Fig. 7, the nodes are fully fixed at the right extremity of the sample thus simulating the clamping of the plate during the JWRI tests while free sliding along x is used along the symmetry line. Treating the liquid material in the weld pool is a tricky problem as commercial mechanical software's are based on a lagrangian description and cannot treat liquid flow. When going through the liquid state, all plastic deformations are reset to zero. But using the *anneal temperature feature in Abaqus 6.8 is impossible with a strain rate dependent mechanical model such as the one described in Eq. 1. Similarly to Wei et al. [27] who used a rebirth technique to model the deposition of a filler material in the weld pool, finite elements reaching the liquidus temperature 1080°C in front of the weld pool are removed from the computation domain. They are later on included without any strain when their temperature falls below 1080°C. As the strain rate is of high interest in the present study, small elements size and time steps are used in order to obtain good spatial and time derivatives of the solid velocity, i.e. in order to obtain a good estimate of the strain rate. The time step is of the order of 0.001 msec. The typical CPU time on a SGI 1.6 GHz server, around 9 hours, remains acceptable and allowed us to run many sensitivity tests.

Two hot tearing (HT) indicators are used in the present study. The first one comes from the analysis of the U ductility curve and is based on the yy component (i.e. the component perpendicular to the thermal gradient) of the viscoplastic strain accumulated in the BTR. This one is assumed to correspond to solid fractions going from 70% (ZST = 1075°C) to 95 % (coalescence temperature of 1050°C) as can be read in Fig. 5. The second HT indicator based on the Rappaz-Drezet-Gremaud [5] is represented by the yy component of the viscoplastic strain rate at a solid fraction close to 95%, i.e. at the coalescence temperature of the CuCrZr alloy. The higher the HT indicator is, the higher the risk to initiate a crack. The

HT indicators are saved only during cooling (i.e. during solidification) at each integration point using the user-subroutine UVARM and only along the weld axis (y = 0) as cracks always initiated along this line. In the rest of the paper, the first indicator is called for simplicity plastic strain and the second one viscoplastic strain rate.

V FINITE ELEMENT RESULTS

This section presents the finite element results concerning the EB welding of the CuCrZr alloy when the width of the sample increases, all other parameters and boundary conditions remaining constant. Sound, i.e. uncracked, JWRI welding tests are presented first to study the values of the HT indicators at the onset of hot tearing. Then, the results obtained with a "cracked" specimen are presented to study the propagation conditions of a hot tear.
Using the material properties and process parameters presented in sections III and IV, the temperature field for a plate width of 30 mm is shown in Fig. 8 when the beam x-position is 60 mm. The weld pool corresponding to temperatures higher than the liquidus temperature of the alloy 1080°C appears in white.
Upon cooling, as all strain components are reset to zero when the "liquid" elements are reactivated, the thermal strain is also reset to zero and decreases to -1.7% at 20°C, as shown in Fig. 9. Indeed, the contraction of the alloy behind the weld pool is partially hindered by the cold part of the plate and leads to tensile strains at the rear of the weld pool that might exceed the ductility limit of the alloy and lead to crack initiation.

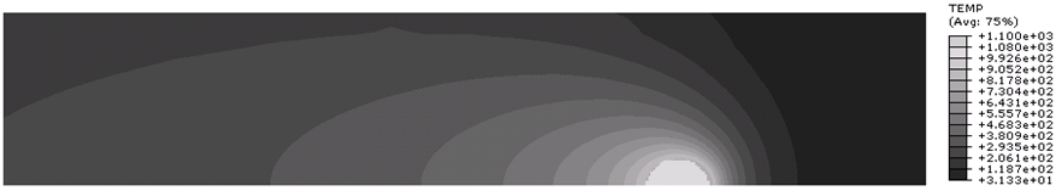

Fig. 8: Temperature distribution when the electron beam is located at x = 60 mm. The weld pool appears in white.

Fig. 9: Thermal strain distribution when the electron beam is located at x = 60 mm.

The distribution along the fusion line of the two HT indicators defined in section IV, i.e. the plastic strain and the plastic strain rate is presented in Fig. 10 and 11, respectively, for three specimen widths, 30 mm, 50 mm and 78 mm. For a given width, the indicators present a

maximum very early in the run-in regime and then decrease over a typical length of 10 mm before entering the on-going zone of welding. The maximum is located very close to x = 0, that is at the location where hot tears initiate. In addition, as the width decreases the maximum plastic strain increases from 0.17 % to 0.27 % and 0.42 %. Similarly, the maximum plastic strain rate increases from 0.1 /s to 0.18 /s and 0.22 /s. As reported in the experimental part, the width of 50 mm is considered as the critical width that leads to hot tearing initiation. Therefore, the critical values for the HT indicators are 0.27 % plastic strain and 0.18 /s plastic strain rate. Please note that in the steady state regime of welding, the HT indicators are much lower than in the run-in. This agrees well with the fact that hot tears, if observed, always initiated in the run-in and never in the on-going zone. The plastic strain of 0.27 % proves that the alloy exhibits a little bit of ductility when reaching the fully solid state. This value is lower than the value found by Kerrouault [17] for a stainless steel. Using the RDG formalism for hot tearing prediction, a plastic strain rate of 0.18 /s yields a cavitation pressure of 84.3 kPa which is comparable to values found for aluminium alloy [5, 10]. Albeit, those critical values depend on the way the plastic flow is extrapolated in the mushy state. In this area, some work is still needed although the major difficulty resides in the very short solidification interval of the alloy, 32°C. In addition, it has been observed that the weld pool gets larger right after the appendice has fallen owing to the presence of a transient thermal regime (cf. Fig. 4). Numerical tests with a higher absorption coefficient (90% over the first 10 mm) in the run-in showed very little influence on the two HT indicators.

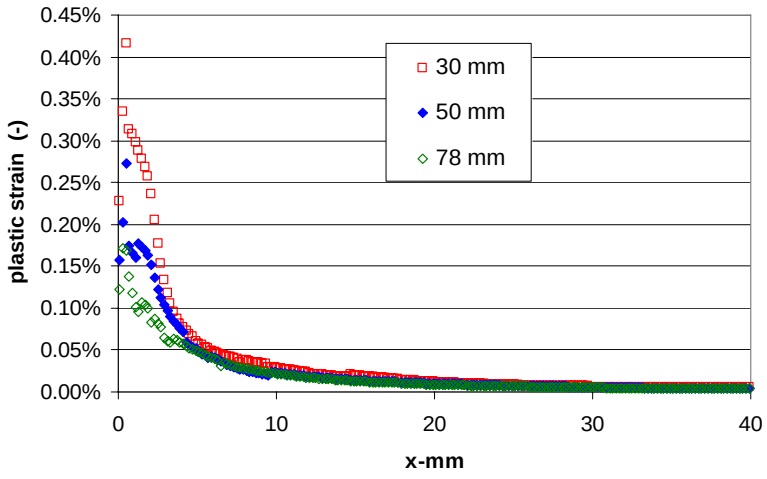

Fig. 10: Distribution of the first HT indicator (plastic strain) along the weld line for three specimen widths.

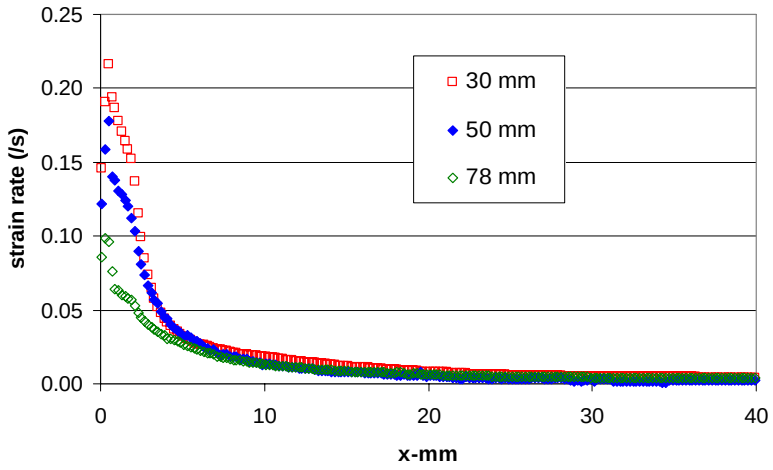

Fig. 11: Distribution of the second HT indicator (plastic strain rate) along the weld line for three specimen widths.

As mentioned before, once a hot tear initiates in the run-in, it simply propagates along the fusion line up the point where it starts to feel the fixtures imposed by the clamping at the other specimen extremity in the vacuum chamber. To study the conditions of propagation of a crack, the FE model is run but this time the mechanical condition applied on the nodes present on the weld line is relaxed at the rear of the weld pool thus simulating the propagation of a crack. This way, each side of the plate is free to either close up thus simulating crack healing or open up thus simulating crack propagation. The situation computed at three instants during run-in is shown in Fig. 12 for a specimen width of 30 mm and with a magnification factor of 5 for better visibility. As the weld beam travels to the right, the sides of the weld seam tend to open up. In addition, the two HT indicators give values very close to zero even in run-in that is way lower than the critical values.

A similar behaviour although with a lower opening is found for a width of 78 mm, for which no crack was observed experimentally (cf. Table 1). This means that when a crack has initiated, it naturally propagates until it meets other mechanical and/or thermal conditions that might heal it. This point stresses the fact that the initiation conditions for a hot tear are much more severe that its propagation conditions. This might explain the great discrepancy present in the literature on the hot tearing sensitivity of metallic alloys, especially when the crack length is considered as an indicator of their sensitivity to solidification cracking.

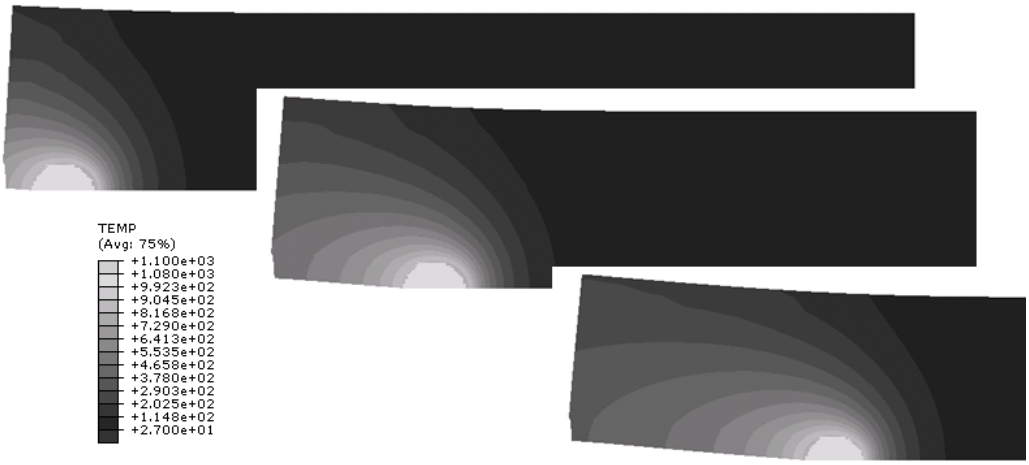

Fig. 12: temperature field over the distorted mesh (displacement magnified by a factor 5) when the nodes are relaxed behind the weld pool simulating the propagation of a hot tear.

CONCLUSION

The initiation conditions of a hot tear in a CuCrZr alloy during electron beam welding are studied by associating experimental tests to a numerical analysis. A threshold of 50 mm in the JWRI specimen width is determined experimentally for the alloy welded at 50 cm/min with a power of 3.5 kW. With the help of a thermo-mechanical model, a critical viscoplastic strain accumulated in the brittle temperature range of 0.27% and a critical viscoplastic strain rate of 0.18 /s at the coalescence temperature are determined. This yields a cavitation pressure of 84.3 kPa. In addition, it is evidenced that the initiation conditions of a hot tear are much more severe than their propagation conditions. This explains why once initiated, a hot crack propagates so easily. The next step in this study is to check the sensitivity of the thresholds to the welding speed and power. In addition, a better description of the mechanical behaviour in the mushy state and the annealing thermal treatment experienced by the alloy in the heat affected zone is also needed. Indeed, both of them might alter the resistance the alloy can oppose to the thermally induced deformations.

APPENDICES AND ACKNOWLEDGEMENTS

We would like to thank the company Le Bronze Industriel which technically and financially supported the work presented here as well as La Région Champagne Ardenne. The Gleeble 3500 machine at Université de Bretagne Sud was co-financed by the European Regional Development Fund (ERDF).

REFERENCES

[1] U. LUCONI, M. DI MARCO, A. FEDERICI, M. GRATTAROLA, G. GUALCO, J.M. LARREA, M. MEROLA, C.OZZANO, G. PASQUALE. *Development of plasma facing components for the domeliner component of the ITER divertor.* Fusion Engineering and Design, Vol. 75-79, 2005, pp. 271-276.

[2] M. LIPA, A. DUROCHER, R. TIVEY, TH. HUBER, B. SCHEDLER, J. WEIGERT: *The use of copper alloy CuCrZr as a structural material for actively cooled plasma facing and in vessel components.* Fusion Engineering and Design, Vol. 75-79, 2005, pp. 469-473.

[3] M. SHIBAHARA, H. SERIZAWA, H. MURAKAWA*: Finite element method for hot cracking analysis using temperature dependent interface element,* Mathematical Modelling of Weld Phenomena, Vol. 5, 2001, pp. 253-267.

[4] V. PLOSHIKHIN, A. PRIKHODOVSKY, A. ILIN, C. HEIMERDINGER, F. PALM: *Mechanical-metallurgical approach for prediction of solidification cracking in welds,* Mathematical Modelling of Weld Phenomena 8, Vol. 8, 2007, pp. 87-105.

[5] P.T. HOULDCROFT: *A simple cracking test for use with argon arc welding,* British Welding Journal, Oct. 1955, pp. 471-475.

[6] M. KATOH, K. NISHIO, S. MUKAE: *A simple comparison of the conventional and reverse Houldcroft type hot cracking tests in A5052 aluminium alloy sheet,* Journal of Japan Welding Society, Vol. 12, n° 2, 1994, pp. 179-185.

[7] F. MATSUDA AND K. NAKATA: *A new test specimen for self-restraint solidification crack susceptibility test of electron beam welding bead,* Transactions of JWRI, Vol. 12, no. 2, 1982, pp. 87-94.

[8] M. RAPPAZ, J.-M. DREZET AND M. GREMAUD. *A new hot tearing criterion,* Metallurgical and materials transaction A, Vol. 30A, February 1999, pp. 449-445.

[9] J. CAMPBELL, CASTINGS, Elsevier, 2003.

[10] J.A. DANZIG AND M. RAPPAZ. *Solidification,* CRC press, 2009.

[11] J.M. DREZET, M.S.-F LIMA, J.D. WAGNIERE, M. RAPPAZ AND W. KURZ. *Crack-free aluminiun alloy welds using a twin laser process*, Proceedings of the Inter. Institute of Welding Conf., Eds. P. Mayr, G. Posch and H. Cerjak, july 2008, pp. 87-94.

[12] D.G. ESKIN, SUYITNO AND L. KATGERMANN. *Mechanical properties in the semi-solid state and hot tearing of aluminium alloys*, Progress in materials science, vol. 49, 2004, pp. 629-711.

[13] J.-M. DREZET AND M. RAPPAZ. *A new hot tearing criterion for aluminium alloys*, Proceedings of the 1st Esaform conf. on material forming, Ecole des mines de Paris, 1998.

[14] T. W. CLYNE AND G. J. DAVIES. *The influence of composition on solidification cracking susceptibility in binary alloy systems*, British Foundrymen, 1981, vol. 74 (4), pp. 65-73.

[15] W. RINDLER, E. KOZESCHNIK AND B. BUCHMAYR. *Computer simulation of the Brittle Temperature Range (BTR) for hot cracking in steels*, Steel Res., 2000, vol. 71 (11),pp. 460-465.

[16] M. RAPPAZ, A. JACOT AND W. J. BOETTINGER. *Last-stage solidification of alloys: theoretical model of dendrite-arm and grain coalescence*, Met. And Mat. Trans. Vol. 34A, March 2003, pp. 467-479.

[17] N. KERROUAULT. *Fissuration a chaud en soudage d´un acier inoxydable austenitique. PhD work*, Ecole centrale de Paris, 2000.

[18] O. CERRI. *Rupture à chaud dans les aciers au cours de leur solidification: caractérisation experimentale et modélisation thermomécanique*, PhD work, Ecole des Mines de Paris, 2006.

[19] M. RAPPAZ, J.M. DREZET, V. MATHIER AND S. VERNÈDE. *Towards a micro-macro model of hot tearing*, presented at ICAA 2006, Vancouver, and published in Materials Science Forum vols. 519-521 (July 2006) pp. 1665-1674, Trans Tech Publications, Switzerland.

[20] M. M'HAMDI, A. MO AND C. L. MARTIN. *Two-phase modeling directed toward hot tearing formation in aluminum direct chill casting*, Met. and Mat. Trans. Vol. 33A, 2002, pp. 2081-2093.
[21] O. LUDWIG, C.-L. MARTIN, J.M. DREZET AND M. SUÉRY. *Rheological behaviour of Al-Cu alloys during solidification: constitutive modelling, experimental identification and numerical study* Met. Mat. Trans, vol 36A, June 2005, p. 1525-1535.
[22] J. WISNIEWSKI. *Modélisation thermomécanique de la fissuration à chaud en soudage par faisceau d'électrons d'un alliage CuCrZr*, PhD work, Univ. de Bretagne Sud, France, 2009.
[23] J. WISNIEWSKI, J.M. DREZET, D. AYRAULT AND B. CAUWE. *Determination of the thermo-physical properties of a CuCr1Zr alloy from liquid state down to room temperature,* Int. J. of Material Forming, Suppl. 1, 2008, pp.1059 –1062.
[24] J. WISNIEWSKI, D. CARRON, M. CARIN, J. COSTA, D. AYRAULT AND P. PILVIN. *Identification du comportement mecanique d'un alliage CuCr1Zr*, Proceedings of Journées annuelles 2009 de la SF2M, Rennes, June 2009.
[25] P. PILVIN. *Notice d'utilisation de SiDoLo*, Université de Bretagne-Sud, Version 2.4495, 2003.
[26] L. KARLSSON. *Thermal stresses in welding*, ed. R. B. Hetnarski, Elsevier, 1986.
[27] Y.-H. WEI, Z.B DONG, R. P. LIU AND Z. J. DONG. *3D numerical simulation of weld solidification cracking*, Modelling and simulation in Mat. Science and Eng., vol. 13, 2005, p. 437-454.